CARDIAC

Marco Francone
Steven Dymarkowski
Maria Kalantzi
Frank E. Rademakers
Jan Bogaert

Assessment of ventricular coupling with real-time cine MRI and its value to differentiate constrictive pericarditis from restrictive cardiomyopathy

M. Francone · S. Dymarkowski ·
M. Kalantzi · F. E. Rademakers ·
J. Bogaert (✉)
Department of Radiology and Cardiology,
Gasthuisberg University Hospital,
Herestraat 49, 3000 Leuven, Belgium
e-mail: Jan.Bogaert@uz.kuleuven.ac.be
Tel.: +32-16-343770
Fax: +32-16-343769

Abstract The purpose of this study was to evaluate the use of respiratory-related ventricular coupling to differentiate patients with constrictive pericarditis (CP) and restrictive cardiomyopathy (RCM). In 18 histologically proven cases of CP, 6 patients with inflammatory pericarditis (IP), 15 RCM patients and 17 normal subjects, real-time cine MRI was performed in the cardiac short-axis (basal half of the ventricles) during operator-guided deep respiration. The images were analyzed for ventricular septal position and shape during early ventricular filling. Early diastolic septal inversion (I) or flattening (F) was found in all CP (I:15,F:3), and in all IP (I:2,F:4), but seldom in normals (F:1) and not in RCM. The septal abnormalities occurred at the onset of inspiration and rapidly disappeared with the next heartbeats. The amount of ventricular coupling was evaluated by quantifying the difference in the maximal septal excursion between inspiration and expiration. This parameter, normalized to the biventricular diameter, was significantly larger in CP (20.0± 4.5%, $P<0.0001$) and IP (14.8±3.2%, $P<0.0001$) patients than in normals (7.0±2.4%), whereas RCM patients had a trend toward decreased excursion (4.2±1.7%, $P=0.11$). A cut-off value of 11.8% (mean normals +2 SD) enabled to differentiate CP patients from normals and RCM patients completely. Real-time cine MRI can easily depict increased ventricular coupling, which may be helpful to better differentiate between CP and RCM patients, especially in patients with normal or minimally thickened pericardium. The increase in coupling in IP patients is likely caused by decreased compliance of the inflamed pericardial layers.

Keywords Magnetic resonance ·
Pericarditis · Constrictive pericarditis ·
Restrictive cardiomyopathy ·
Ventricular coupling · Cardiac physiology

Introduction

The hallmark of constrictive pericarditis (CP) is increased pericardial stiffness, leading to impaired ventricular filling with a subsequent rise in filling pressures [1]. The diagnosis of CP and differentiation from other entities with increased filling pressure, such as restrictive cardiomyopathy (RCM), remain difficult. Although pericardial thickening (i.e., pericardial width of more than 4 mm) has been used as a morphological criterion to diagnose CP, it has

been shown recently that a significant number of patients with pericardial constriction at surgery had a minimally increased (<4 mm) or even a normal pericardial width [2, 3]. Analysis of the cardiac inflow patterns and evaluation of the impact of respiration on the inflow curves with Doppler echocardiography allows to assess the hemodynamics in patients with suspected CP directly [4]. Respiration, however, interferes with the position of the area of interest within the valvular orifice, and thus with the obtained flow profile, and can cause false-positive results. A

third useful criterion to differentiate CP from RCM is the early diastolic "septal bounce or septal notch" phenomenon, reflecting pathologic ventricular coupling, using echocardiography or MRI [5, 6]. In CP patients this ventricular coupling is increased, while it is normal in RCM patients. We recently described a novel approach to assess the ventricular septal motion, shape and excursion in real-time by means of fast cine MRI techniques [7]. The present study was undertaken to define quantitative measures of ventricular septal motion patterns and total septal excursion during respiration in normal subjects, patients with RCM, patients with inflammatory pericarditis (IP) and patients with surgically and histologically proven CP. We sought to evaluate whether cut-off values could be determined useful in the diagnosis of CP.

Materials and methods

Study population

The patient population included 18 CP (9 females, 63±16 years) and 15 RCM (8 females, 64±15 years) patients (Table 1). All patients had objective evidence of impaired cardiac filling and were referred for MRI to rule out CP. The final diagnosis of CP was made on surgical and histological grounds (end-stage chronic fibrosing pericarditis: ten; mixed inflammatory-constrictive pericarditis: seven; pericardial sclerosis: one). Pericardial calcifications were found histologically in eight patients. The diagnosis of RCM was based on impaired cardiac filling (e.g., increased filling pressures and no echo-Doppler evidence of respiratory-dependent ventricular coupling) in combination with the absence of pericardial thickening on MRI. Endomyocardial biopsy was performed in 10/15 RCM patients and showed amyloid depositions in 5 and non-specific findings in 5. As control groups for MRI, we included 17 normal subjects (7 females, 50±16 years) and 6 patients with clinical and laboratory evidence of inflammatory pericarditis (3 females, 55±7 years). All studies were performed according to the guidelines of the hospital committee on medical ethics and clinical investigation and all subjects gave informed consent for the study.

MRI protocol

All MRI studies were performed on a 1.5-T Intera MRI unit (Philips Medical Systems, Best, The Netherlands) with Powertrak 6,000 gradients (30 mT/m, 220 μs rise time), a dedicated cardiac software package and the standard five-element Synergy cardiac coil and VectorCardioGram (VCG) triggering. Assessment of ventricular coupling with real-time cine MRI was part of a comprehensive evaluation. Imaging started with scout views to localize the heart and continued with real-time cine MRI to determine the cardiac imaging plane positions interactively. Cardiac and pericardial morphology was studied using breath-hold T1-weighted fast spin-echo MRI in the axial and the cardiac short-axis planes. In patients with clinical suspicion of inflammatory pericarditis, an additional T2-weighted short-tau inversion-recovery (STIR) fast spin-echo MRI acquisition was performed. Cardiac function was evaluated using balanced steady-state free-precession (SSFP) cine

Table 1 Patient and volunteer data

	Normals	CP	IP	RCM
Number	17	18	6	15
Male/female	10/7	9/9	3/3	7/8
Age (years)	50±16	63±16	55±7	64±15
RV pressure (mm Hg)	–	19±6	–	17±5
LV pressure (mm Hg)	–	23±7	–	22±5
Pericardial thickness (mm)	1.6±0.6	7.6±5.5	12±4.2	2.9±1.5
	(0.8–3)	(1.5–12)	(8–20)	(1.5–6)
Biventricular diameter (mm)				
At inspiration	9.2±1.1	8.2±1.3	9.3±0.8	9.1±1.3
At expiration	9.1±1.1	8.1±1.0	9.0±1.0	9.0±1.3
Inspiratory septal shape				
Normal	16	0	0	15
Flattened	1	3	4	0
Inverted	0	15	2	0
Absolute septal excursion (mm)	6.6±2.6	17.5±4.0	15.5±4.2	4.4±2.0
Normalized septal excursion (%)	7.0±2.4	20.0±4.5	14.8±3.2	4.2±1.7
	(0.9–10.6)	(12.6–28.3)	(11.5–19.4)	(1.4–7.5)

The range of values is shown between brackets. Ventricular pressures measured by cardiac catheterization
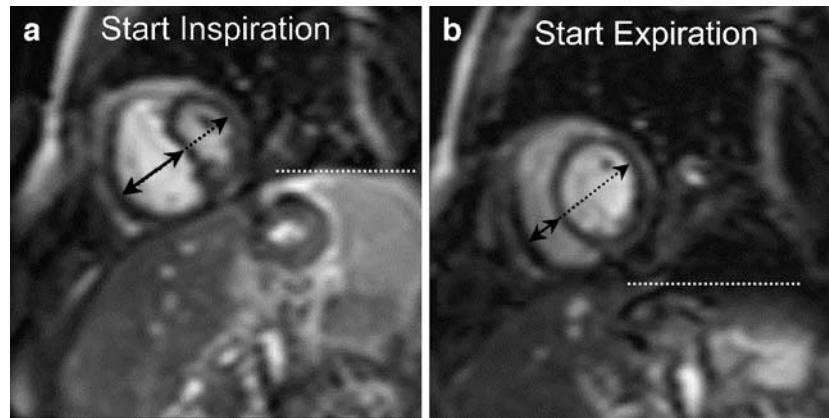
Fig. 1 Analysis of respiratory-related septal excursion. The relative position of the septum can be obtained by dividing the distance between RV free wall and septum (*full line*) by the biventricular distance (*dashed line*). If done during inspiration and expiration, at early ventricular filling, the respiratory-related septal excursion can be quantified. The *horizontal dashed white line* indicates the position of the left hemidiaphragm, which is used to determine the phase of the respiratory cycle. In this patient with CP, paradoxical septal inversion was visible at the onset of inspiration, with enhanced right-sided excursion during onset of expiration. The relative septal position at end-inspiration is 56.6% and 31.0% at end-expiration, giving a relative septal excursion of 25.6%

MRI in the intrinsic cardiac axes. Real-time, non-triggered cine MRI, using the balanced-SSFP technique in combination with parallel imaging, was then performed in the cardiac short-axis in the basal half of the ventricles. During data acquisition, the operator instructed the patients and normal subjects to breathe deeply in and out. The temporal resolution was 64 ms with a spatial resolution of 2.81×2.78 mm (reconstructed pixel size). With a total of 300 shots, the total imaging period was approximately 20 s, covering at least three complete respiratory cycles. In order

Fig. 2 Constrictive pericarditis in a 28-year-old male patient. **a** T1-weighted axial fast spin-echo MRI shows diffuse pericardial thickening (*arrows*), which is most pronounced over the right ventricle. The pericardium has a hypo-intense signal and is irregularly defined. **b** Short-axis real-time cine MRI during operator-guided breathing shows abnormal septal motion with septal inversion during onset of inspiration (*arrow* in *upper row*). The abnormal septal motion rapidly disappears, while during expiration an increased rightward motion is noticed (*arrow* in *lower row*). The respiratory-related septal excursion was 25.6%. All images shown were obtained at the moment of early ventricular filling. The *dashed white line* represents the end-inspiratory position of the diaphragm
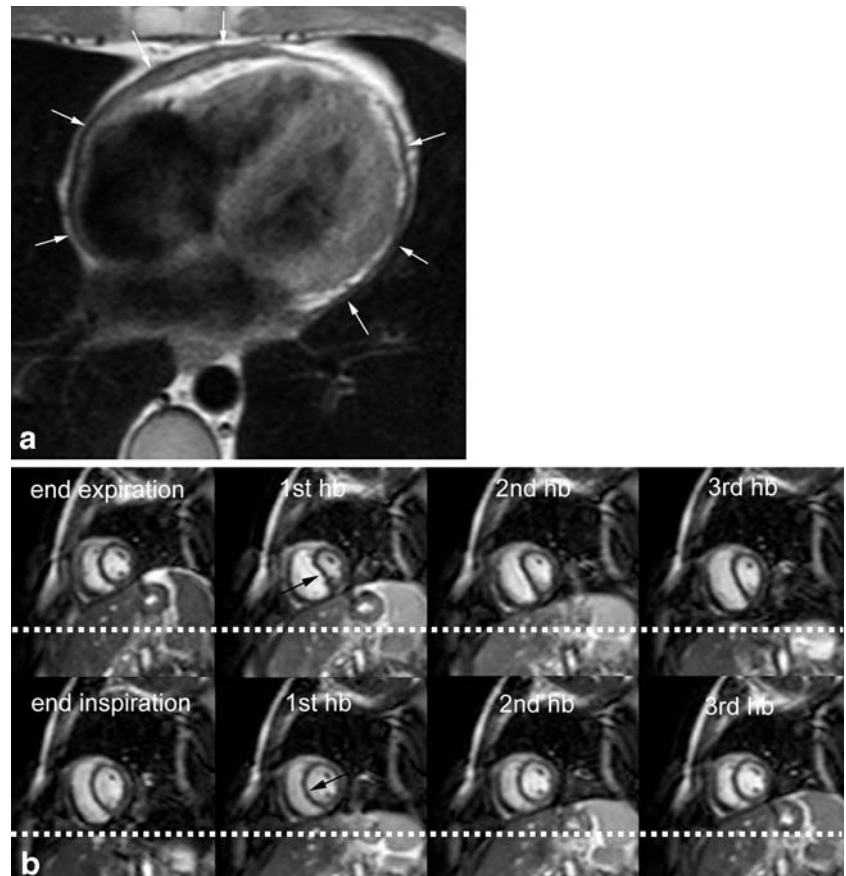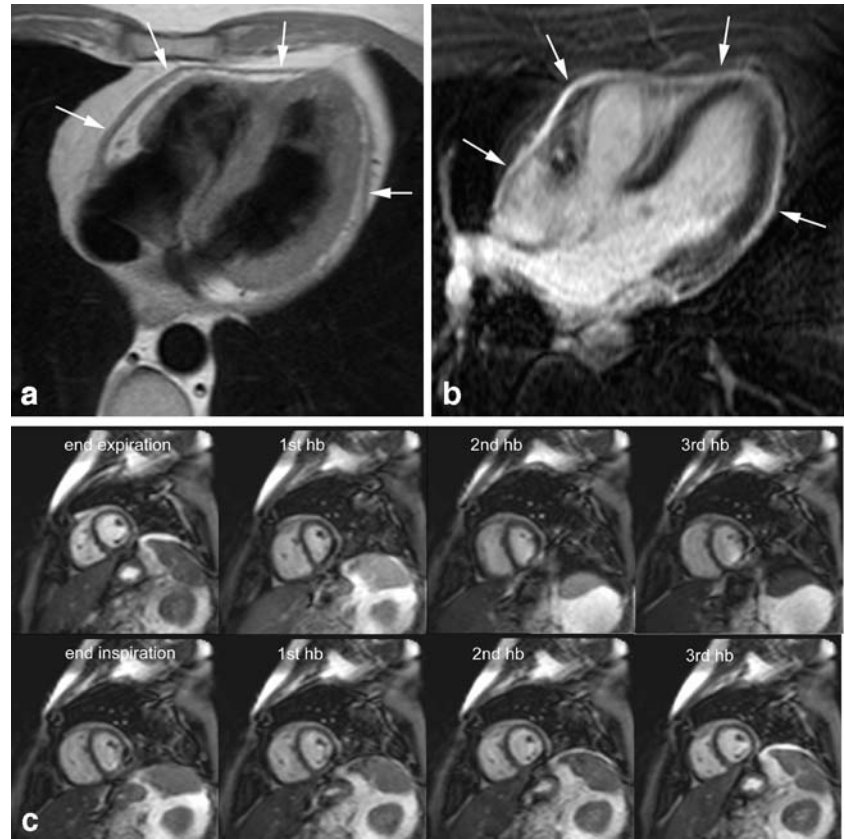
Fig. 3 Inflammatory pericarditis in 45-year-old male patient. **a** T1-weighted axial fast spin-echo MRI shows diffuse thickening of the pericardium (*arrows*). The pericardial signal is nearly iso-intense to the signal of myocardium tissue. On the axial post-contrast images using the contrast-enhanced inversion-recovery MRI technique with additional fat suppression (**b**), a strong enhancement of the pericardium is found (*arrows*). **c** Short-axis real-time cine MRI during operator-guided breathing shows septal flattening during onset of inspiration. The flattening disappears during the subsequent heart beats. The respiratory-related excursion is 14.1%. All images shown were obtained at the moment of early ventricular filling

to obtain good patient cooperation and a successful study, the different procedures were explained and instructed to the patient prior to the MRI study.
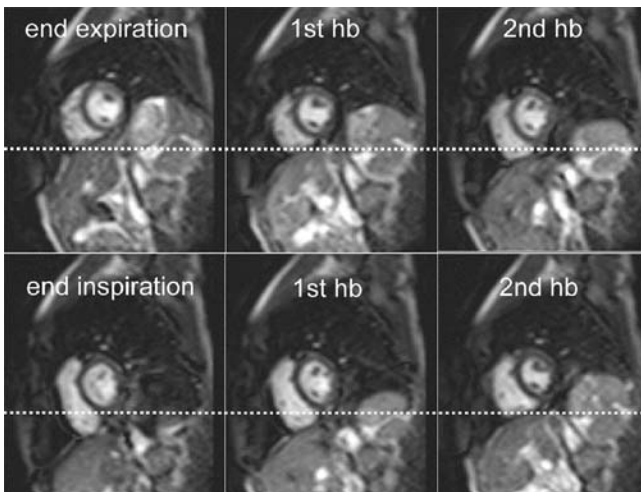

Fig. 4 Normal volunteer. Short-axis real-time cine MRI during operator-guided breathing shows no shape changes of the ventricular septum. The respiratory-related excursion is 7.1%. The *dashed white line* represents the end-inspiratory position of the diaphragm

Data analysis

Analysis of the MR images included morphological assessment of the pericardium (i.e., thickness, localization, extent and tissue characterization), myocardium (i.e., thickness, tissue characterization) and global cardiac and venous morphology. Functional analysis included the assessment of ventricular systolic function. To obtain information about the ventricular coupling, the cardiac short-axis real-time cine MR images were visually analyzed for abnormal motion and shape changes of the ventricular septum throughout the cardiac and respiratory cycle. Since abnormal ventricular coupling in CP occurs during early ventricular filling, we specially focused our data analysis to this phase of the cardiac cycle. The shape of the ventricular septum at early diastole was defined as normal (i.e., convex to the right), flattened or inverted (i.e., convex to the left). Next, the respiratory-related septal excursion was quantified. This was achieved by measuring the distance using a horizontal long-axis plane between the right ventricular (RV) free wall and septum, as well as the biventricular diameter using the same plane (Fig. 1). During inspiration this was done for the heartbeat showing the largest septal displacement to the left. During expiration, the same was done for the largest displacement to the right. The above measurements provide objective data about the position of the ventricular septum

in relation to both ventricles and allow the calculation of the respiratory-related, absolute as well as normalized septal excursion. Absolute septal excursion (expressed in millimeters) can be calculated by subtracting the RV-wall to septum distance in inspiration from the distance during expiration. Use of normalized distances, however, is preferable because distances are corrected for the differences in ventricular dimensions. These were obtained by dividing the RV-wall to septum distance by the biventricular diameter at inspiration and expiration, respectively. This yields a percent septal shift. Although we were not able to use a synchronous acquisition of the ECG and breathing pattern in the present study, the phase of the respiratory cycle could be achieved easily using a visual assessment of the up- and downward motion of the diaphragm on the cardiac short-axis real-time cine MR images. In this way, end-expiration and end-inspiration, onset of inspiration and expiration, as well as depth of inspiration, could be well

determined in all subjects. A similar visual analysis was used to assess the exact phase of the cardiac cycle. A temporal resolution of 64 ms is sufficiently fast to acquire all important phases of the cardiac cycle. Early diastole usually coincided with the 2–3 image after end-systole (defined as the smallest ventricular cavity). All data are shown as mean±SD. For the statistical analysis and comparison of the different groups we used an ANOVA test with the Scheffé post-hoc test.

Results

The maximal pericardial thickness in CP patients (7.6± 5.5 mm, range 1.5–24 mm) was significantly larger than in normal subjects (1.6±0.6 mm, range 0.8–3.0 mm, $P<0.0001$) and RCM patients (2.9±1.5 mm, range 1.5–6 mm, $P<0.0001$), but not different from IP patients (12±4.2 mm, range 8–
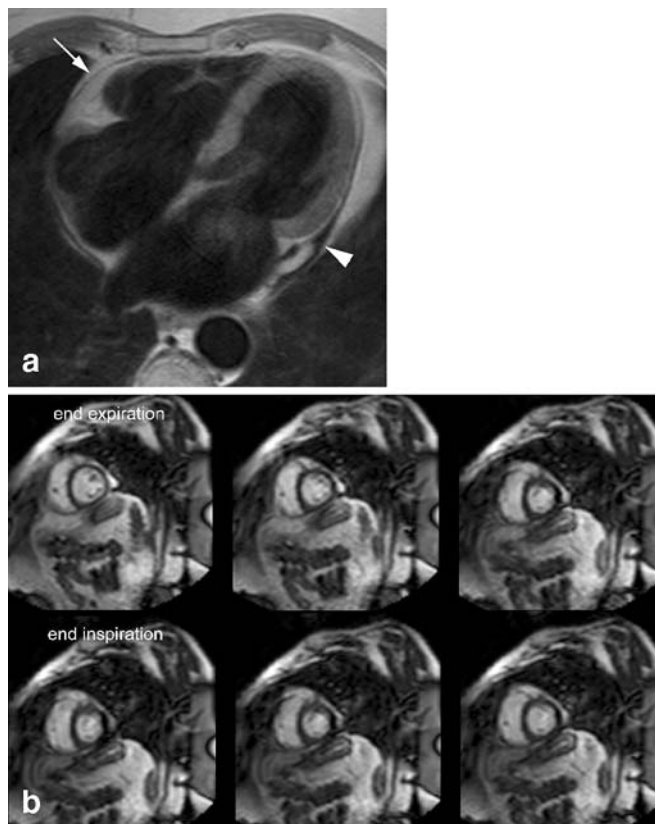

Fig. 5 Primary restrictive cardiomyopathy in 72-year-old female patient. **a** T1-weighted axial fast spin-echo MRI shows normal pericardial thickness (1.5 mm) (*arrow*), except of a small pericardial effusion over the left atrioventricular groove (*arrowhead*). **b** Short-axis real-time cine MRI during operator-guided breathing shows no shape changes of the ventricular septum. The respiratory-related excursion is 6.3%. All images shown were obtained at the moment of early ventricular filling
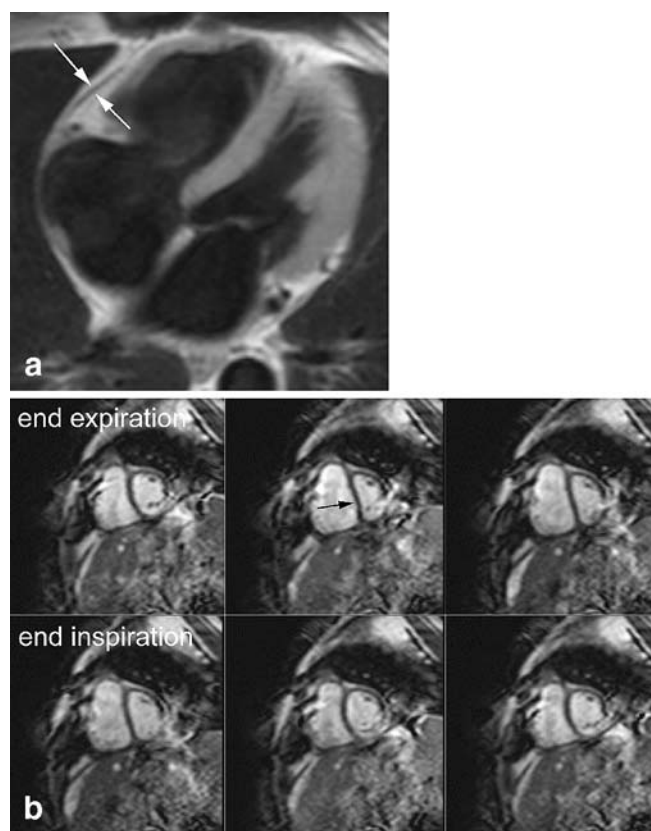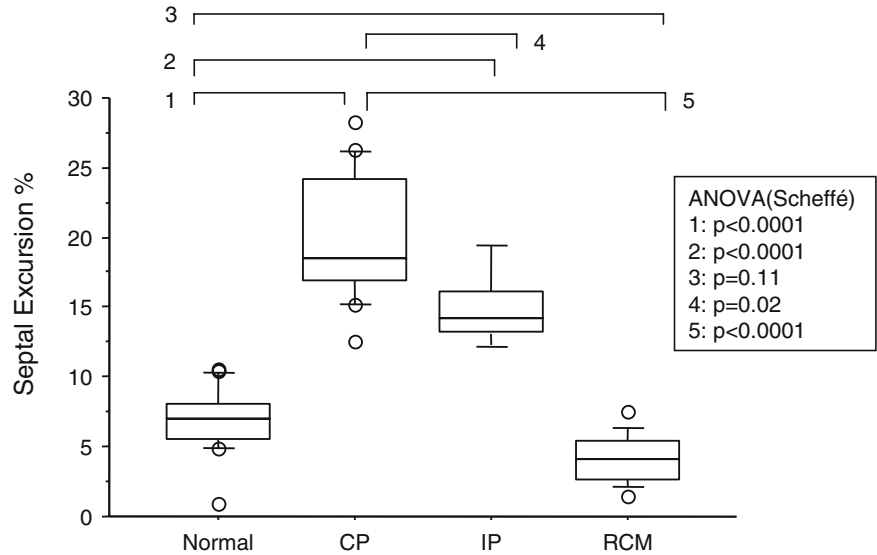

Fig. 6 Non-thickened constrictive pericarditis in 75-year-old male patient. **a** T1-weighted axial fast spin-echo MRI shows a pericardium with a maximal thickness of 2.5 mm (*arrow*). **b** Short-axis real-time cine MRI shows inspiratory septal flattening at onset of inspiration (*arrow*). The septal abnormalities have completely disappeared by the end of inspiration. The respiratory-related excursion is 18.4%. All images shown were obtained at the moment of early ventricular filling. During pericardiectomy, a stiff pericardium was found with mainly pericardial sclerosis and limited amount of fibrosis at histology. Immediately after pericardiectomy, the cardiac increased from 1.7 l/min to 7.5 l/min

Fig. 7 Differences in normalized septal excursion between normal subjects, IP, CP and RCM patients

20 mm, *P*=0.06) (Table 1). In the CP group, the pericardium on the right side of the heart was most frequently involved (*n*=9); less frequently diffuse pericardial thickening was noticed (*n*=5). The remaining four CP patients had a pericardial thickness less than 4 mm (i.e., 1.5, 1.8, 2 and 2.5 mm, respectively) and thus morphologically were not considered as having an abnormal thickened pericardium. Inspiratory, leftward septal motion with septal flattening or inversion during early ventricular filling was invariably present in CP patients, and also in IP patients, but less pronounced (Table 1). This phenomenon was always most pronounced on the first heartbeat after the onset of inspiration and gradually disappeared over the next 1–2 heartbeats (Figs. 2 and 3). Inspiratory septal flattening was found in only 1/17 normals, and never in RCM patients (Figs. 4 and 5). In contrast, all four patients with non-thickened CP presented inspiratory septal inversion (Fig. 6). The septal inversion during expiration was best appreciated on cine loop viewing of the real-time MRI studies (not shown).

Although the biventricular diameter measured at inspiration and expiration in the CP group was slightly smaller than in normals and in the other patient groups, no statistical significance was reached (Table 1). Quantification of the maximal septal shift between inspiration and expiration yielded significantly increased values (both absolute and normalized values) in the CP and IP group compared with normal subjects and RCM patients (Table 1 and Fig. 7). The increase in septal excursion, however, was significantly larger for the CP group than the IP group. RCM patients showed a trend toward decreased septal excursion compared with normals (*P*=0.11). Using a cut-off value of 11.8% (mean normal subjects +2 SD) enabled to differentiate between normals and CP patients. This cut-off value was also useful to differentiate between RCM and CP patients.

Discussion

In the present study, real-time cine MRI during operator-guided breathing demonstrated increased ventricular coupling in CP, and to a lesser extent also in IP patients, as evidenced by an early diastolic septal inversion or flattening at the onset of inspiration, and an increased total respiratory shift. In contrast, RCM patients showed no respiratory-related changes in ventricular septal shape and a trend toward decreased respiratory-related septal excursion compared with normals. This real-time MRI sequence, which takes only about 20 s, provides highly valuable information about the influence of respiration on ventricular filling. It can be easily incorporated into existing MRI protocols to study patients with clinical suspicion of CP. Also in other diseases with abnormal ventricular coupling, such as patients with cor pulmonale due to pulmonary emboli, real-time cine MRI may be valuable to depict the normalization of the ventricular septal shape and motion after thrombo-embolectomy.

Ventricular coupling (or ventricular interdependence) is a normal physiological phenomenon, reflecting the alteration in function of one ventricle due to changes in filling or loading conditions of the other [8]. Inspiration enhances early right ventricular filling while the opposite occurs during expiration. This leads to a small septal excursion in normal subjects, and in a minority of them to inspiratory septal flattening dependent also on the depth of respiration. In CP patients, the reduction in pericardial compliance results in a pathological ventricular coupling [9]. During early RV filling, which precedes LV filling, the outward expansion is impaired by the pathological pericardium, resulting in a sudden rise of the RV pressure, and as a consequence a sudden leftward shift with flattening or inversion of the ventricular septum. This phenomenon is

strongly influenced by the respiratory cycle. Real-time cine MRI has a sufficiently high temporal resolution to study both the cardiac- and respiratory-related variation. In the present study, the septal abnormalities always occurred at the onset of ventricular filling and disappeared later in diastole. Moreover, it always coincided with the onset of inspiration with abnormalities being most pronounced in the first heartbeat, and rapidly diminishing in intensity during the following heartbeats. During expiration, an opposite phenomenon was noticed with an increased rightward septal shift due to enhancement of the LV filling. As a consequence, the respiratory-related septal excursion is significantly increased in CP patients. In RCM patients, the normally compliant pericardium does not limit inflow, while their restrictive physiology, caused by decreased myocardial compliance, affects both ventricles. In none of these patients was septal flattening or inversion found. RCM patients showed a trend toward decreased respiratory-related septal excursion, which is likely related to the increased myocardial stiffness, impeding septal motion during diastole.

The importance of assessing pathological ventricular coupling is shown in the four patients with non-thickened CP who would have been misdiagnosed on MRI if only morphological criteria (i.e., pericardial thickness) were used. Use of a cut-off point, in the present study defined as mean normal subjects ±2 SD, enables to distinguish between those with and without decreased pericardial compliance. However, it should be emphasized that this respiratory-related pathological coupling is not exclusively found in CP, nor is it obligatorily present in all CP patients. In IP patients, the inflammatory thickened pericardial layers may decrease the pericardial compliance and lead to a transient pericardial constriction [10]. Moreover, many patients with inflammatory pericarditis will evolve toward a constrictive pericarditis, and histology often shows a mixture of inflammation and granulation tissue in these patients. As a consequence, differentiation between CP and IP based on the assessment of ventricular filling is often not possible. However, the use of the pericardial signal intensity on T1- and T2-weighted spin-echo MRI and the enhancement of the pericardial layers after contrast administration are usually adequate to assess underlying pericardial inflammation. Other diseases, such as cor pulmonale, may also lead to septal inversion. In these patients, the septal inversion, however, is minimally influenced by the respiration, and the inversion is usually present throughout the respiratory cycle. Conversely, increased ventricular coupling in CP patients is primarily caused by decreased compliance of the pericardium overlying the right ventricle, which is found in the majority of CP patients. However, in a minority of CP patients, such as those with pericardial abnormalities over the left ventricle or with abnormalities located at the atrioventricular grooves, abnormal septal excursion may be absent [11]. The best imaging plane to study the ventricular septal motion is the short-axis imaging, because abnormalities in septal shape and motion can be directly related to the position of the diaphragm. Although during respiration some through-plane motion may occur (i.e., the short-axis position during inspiration is not the same as during expiration), the septal abnormalities are not limited to a small area of the ventricular septum, but usually involve the basal two thirds of the septum.

In conclusion, inspiratory septal flattening or inversion in combination with increased respiratory-related excursion of the ventricular septum in a patient with clinical evidence of impaired cardiac filling is highly suspect of CP, even in the presence of a normal or near normal pericardial thickness. Although Doppler echocardiography is still the first in-line imaging modality used to study patients with clinical suspicion of CP, because of its capability to assess cardiac diastolic (dys)function as well as septal abnormalities during respiration, MRI has recently become increasingly important [12–14]. Integration of real-time MRI in current MRI protocols will further enlarge its clinical role. MRI combines superb morphological with functional information on the presence and concomitant impact of pericardial abnormalities on the heart and can be of help in the often difficult differentiation between CP and RCM. Moreover, in CP patients, the extent of pericardial abnormalities on MRI can be used to guide the cardiac surgeon's intervention.

References

1. Spodick DH (1997) The Pericardium: a Comprehensive Textbook. M. Dekker, New York, NY, 233,464
2. Sechtem U, Tscholakoff D, Higgins CB (1986) MRI of the abnormal pericardium. Am J Roentgenol 47:245–252
3. Talreja DR, Edwards WD, Danielson GK et al (2003) Constrictive pericarditis in 26 patients with histologically normal pericardial thickness. Circulation 108:1852–1857
4. Hatle LK, Appleton CP, Popp RL (1989) Differentiation of constrictive pericarditis and restrictive cardiomyopathy by Doppler echocardiography. Circulation 79:357–370
5. Hancock EW (2001) Differential diagnosis of restrictive cardiomyopathy and constrictive pericarditis. Heart 86:343–349

6. Giorgi B, Mollet NR, Dymarkowski S, Rademakers F, Bogaert J (2003) Assessment of ventricular septal motion in patients clinically suspected of constrictive pericarditis, using magnetic resonance imaging. Radiology 228:417–424

7. Francone M, Dymarkowski S, Kalantzi M, Bogaert J (2005) Real-time cine MRI of ventricular septal motion. A novel approach to assess ventricular coupling. J Magn Reson Imaging 234:542–547

8. Guzman PA, Maugham WL, Yin FCP et al (1981) Transseptal pressure gradient with leftward septal displacement during the Mueller manoeuvre in man. Br Heart J 46:657–662

9. Santamore WP, Bartlett R, Van Buren SJ, Dowd MK, Kutcher MA (1986) Ventricular coupling in constrictive pericarditis. Circulation 74:597–602

10. Haley JH, Tajik AJ, Danielson GK, Schaff HV, Mulvagh SL, Oh JK (2004) Transient constrictive pericarditis: causes and natural history. J Am Coll Cardiol 43:271–275

11. Hasuda T, Satoh T, Yamada N et al (1999) A case of constrictive pericarditis with local thickening of the pericardium without manifest ventricular interdependence. Cardiology 92:214–216

12. Rienmüller R, Gürgan M, Erdman E, Kemkes BM, Kreutzer E, Weinhold C (1993) CT and MR evalution of pericardial constriction: a new diagnostic and therapeutic concept. J Thorac Imaging 8:108–121

13. Masui T, Finck S, Higgins CB (1992) Constrictive pericarditis and restrictive cardiomyopathy: evaluation with MR imaging. Radiology 182:369–373

14. Bogaert J, Dymarkowski S, Taylor AM (2005) Pericardial Disease in Clinical Cardiac MRI. Springer, Berlin Heidelberg New York, 294–300